Islamic Azad University
Mashhad Branch

Peyman Afzal et al. / Iranian Journal of Earth Sciences 5 (2013) / 100-110

Separation of Geochemical Anomalies Using Factor Analysis and Concentration-Number (C-N) Fractal Modeling Based on Stream Sediments Data in Esfordi 1:100000 Sheet, Central Iran

Peyman Afzal[*1], Afshar Zia Zarifi[2], Behnam Sadeghi[1]

1. Department of Mining Engineering, South Tehran Branch, Islamic Azad University, Tehran, Iran
2. Department of Mining Engineering, Lahijan Branch, Islamic Azad University, Tehran, Iran
Received 8 August 2013; accepted 29 September 2013

Abstract

The aim of this study is separation of Fe_2O_3, TiO_2 and V_2O_5 anomalies in Esfordi 1:100,000 sheet which is located in Bafq district, Central Iran. The analyzed elements of stream sediment samples taken in the area can be classified into 5 groups (factors) by factor analysis. The Concentration–Number (C-N) fractal model was used for delineation of the Fe2O3, TiO2 and V2O5 thresholds. According to the thresholds, the distribution of elemental concentration for Fe_2O_3 and TiO_2 were divided to four classifications and V2O5 has five geochemical populations in the area. Based on correlation between obtained results with geological and remote sensing data, the results show that the major anomalies of Fe_2O_3, TiO_2 and V_2O_5 and related factor are mostly situated around granitic/rhyolitic rocks, iron alterations and along faults.

Keywords: *Factor Analysis, Concentration-Number (C-N) Fractal Model, Esfordi, Stream Sediment.*

1. Introduction

The definition of geochemical anomalies from backgrounds is important for interpretation of geological evolution and the ore-forming processes [1, 2, 3, 4]. Mineral exploration based on stream sediment data has been widely utilized for various types of ore deposits" and separation of geochemical anomalies based on stream sediment data is an essential stage to outline discoveries and prospects for mineral exploration [5, 6, 7]. There have been some classical statistics methods for definition of geochemical anomalies from background such as histogram analysis, box plot, summation of mean and standard deviation coefficients and median [8, 9, 10, 11, 12, 13, 14]. The statistical methods consider only the frequency distribution of the elemental concentration paying no attention to spatial variability; the information about the spatial correlation is not always available. Additionally, these methods are only appropriate to cases where geochemical data follows a normal distribution [3, 15, 16, 17, 18].

Fractal/multifractal modeling, established by Mandelbrot (1983), have been widely applied in different branches of geosciences since 1980s [19, 20, 21, 22]. Bolviken et al. (1992) and Cheng et al. (1994) proved geochemical patterns of various elements have fractal dimensions [22, 23].

Several fractal models have been proposed in geochemical data analysis including Concentration-Area (C-A) by Cheng et al. (1994), Number-Size (N-S) by Mandelbrot (1983), Concentration-Distance (C-D) by Li et al. (2003), Concentration-Volume (C-V) by Afzal et al. (2011) and Concentration-Number (C-N) by Hassanpour and Afzal (2013) [4, 22, 24, 25, 26]. Moreover, Studies on many cases revealed that geochemical data could have a multifractal nature [5, 27, 28, 29, 30, 31, 32, 33]. Geochemical data including lithogeochemical, stream sediments and in-situ soil have a multifractal nature which represents differences in geological factors such as alterations, rock units, geochemical and mineralization processes [22, 31, 34, 35, 36, 37, 38, 39].

Multivariate statistical analysis specifically factor analysis is proper techniques to classify and reduce the number of geochemical variables. Factor analysis, as one of the methods of multivariate analysis, has been widely used for interpretation of stream sediment geochemical data. The principal aim of factor analysis is to explain the variations in a multivariate data set by a few factors as possible and to detect hidden multivariate data structures. Factor analysis is suitable for analysis of the variability inherent in a geochemical data set with many analyzed elements. Consequently, factor analysis is often applied as a tool for exploratory data analysis [14, 37, 40, 41].

The purpose of this study was to use the application of C-N fractal modeling and factor analysis to distinguish factors based on Fe2O3, TiO2 and V2O5

---
*Corresponding author.
E-mail address (es): p_afzal@azad.ac.ir

geochemical anomalies for further mineral exploration in Esfordi 1:100000 sheet, Central Iran.

2. Methodology

2.1. C-N fractal model

The N–S model, which was introduced by Mandelbrot (1983), can be employed to demonstrate the distribution of geochemical populations without pre-processing of data [22]. The model shows that there is a relationship between desirable attributes (e.g., ore element) and their cumulative numbers of samples of the elemental concentrations in this studied area. Agterberg (1995) proposed a multifractal model titled Size-Grade for determination of the spatial distributions of giant and super-giant mineral deposits [21]. Monecke et al. (2005) utilized the N-S fractal model to describe element enrichments accumulated with metasomatic processes during the formation of hydrothermal ores in the Waterloo Australia massive sulfide deposit [42]. A power-law frequency model has been intended to describe the N-S relationship according to the frequency distribution of elemental concentrations and cumulative number of samples with those attributes [5, 43, 44, 45, 46, 47, 48, 49]. Hassanpour and Afzal (2013) developed the N-S model and proposed concentration-number (C-N) model. The model is expressed by the following equation [4, 5, 22]:

$$N(\geq\rho) = F\rho - D \quad (1)$$

where ρ indicates element concentration, $N(\geq\rho)$ denotes cumulative number of samples with elemental concentration values greater than or equal to ρ, F is a constant and D is the scaling exponent or fractal dimension of the distribution of elemental concentrations. Log-log plots of $N(\geq\rho)$ versus ρ show straight line segments with different slopes −D corresponding to different concentration intervals [4, 5].

2.2. Factor analysis

Factor analysis is one of the most popular multivariate analysis which is determined as a powerful implement to visualize high dimensional data in lower dimensional spaces based on variance and covariance matrix. It is a useful tool for combining several correlated variables into a single variable, and hence for reducing the dimensionality of datasets into uncorrelated principal components based on covariance or correlations of variables which represents the inter-relationships among the multi-dimensional variables [14, 50, 51]. A large dataset of geochemical variables could be combined in a few factors by this method. Factors could be illustrative of the geological and mineralization processes that generate the correlations among these variables (elemental concentrations) [52, 53].

3. Geological Setting

The Central Iran structural zone includes the Anarak-Bafq-Kerman metallogenic belt, parts of the Uremia-Dokhtar volcanic belt and Sanandaj-Sirjan structural-metamorphic zone. There are mineralization of different types of iron ores (> 2 Gt) which are located in the Bafq district region. The largest reserve of iron ore ever discovered in Bafq district is the Chadormalu mine which contains 400 Mt of iron ore [54, 55, 56].

The Esfordi 1:100000 sheet is one of the most important of geological maps in the Bafq district. The Bafq region is one of the most essential mineralized zones of central Iran with the upper Precambrian metamorphic-sedimentary rocks and Rift series of Precambrian - Paleozoic [54, 55]. Central Iran is a portion of Gondwana land with a Precambrian basement. Within a Pan-African rift zone a huge Infracambrian volcanic field was formed on top of a silicic diapir, with ignimbritic cauldrons, ring fracture intrusions, and resurgent granites (Figs 1) [56, 57].

Intrusive rocks host of magnetite; apatite-magnetite and sometimes they are also rich with Rare Earth Elements (REEs) mineralization. The mineralized zones are commonly associated with calc–alkaline volcanic rocks and metasomatic alteration. Iron oxide–apatite deposits and occurrences occur within felsic volcanic tuffs and volcano-sedimentary sequences of the Early Cambrian age [58, 59]. The magnetite–apatite deposits comprise several orebodies with large-scale replacement and brecciation textures, and a sodic–calcic alteration envelope [58]. The previous studies show that the genesis of the iron ores are similar to Kiruna-type deposits [56, 57]. There are many large and rich iron and iron-apatite deposits and occurrences around the Bafq region, e.g., Chadormalu, Choghart, Seh-Chahoon and Chah-Gaz iron ores and the Esfordi iron-apatite ore deposits (Fig 1).

4. Discussion

In this study, 843 collected stream sediment samples were analyzed by ICP-MS for 34 elements and oxides which correspond to iron mineralization (Fig. 2). Statistical results indicate that Fe2O3, TiO2 and V2O5 mean values are 5.66%, 0.796% and 86.2 ppm, respectively (Table 1). Their histograms have not normal distribution, as depicted in Fig. 3. Based on the elemental distribution, median is assumed to be equal to threshold values [9, 15]. The obtained thresholds are 5%, 0.78% and 77 ppm for Fe2O3, TiO2 and V2O5 respectively. The elemental distributions were built up by IDW estimation method in the area using RockWorks software package.

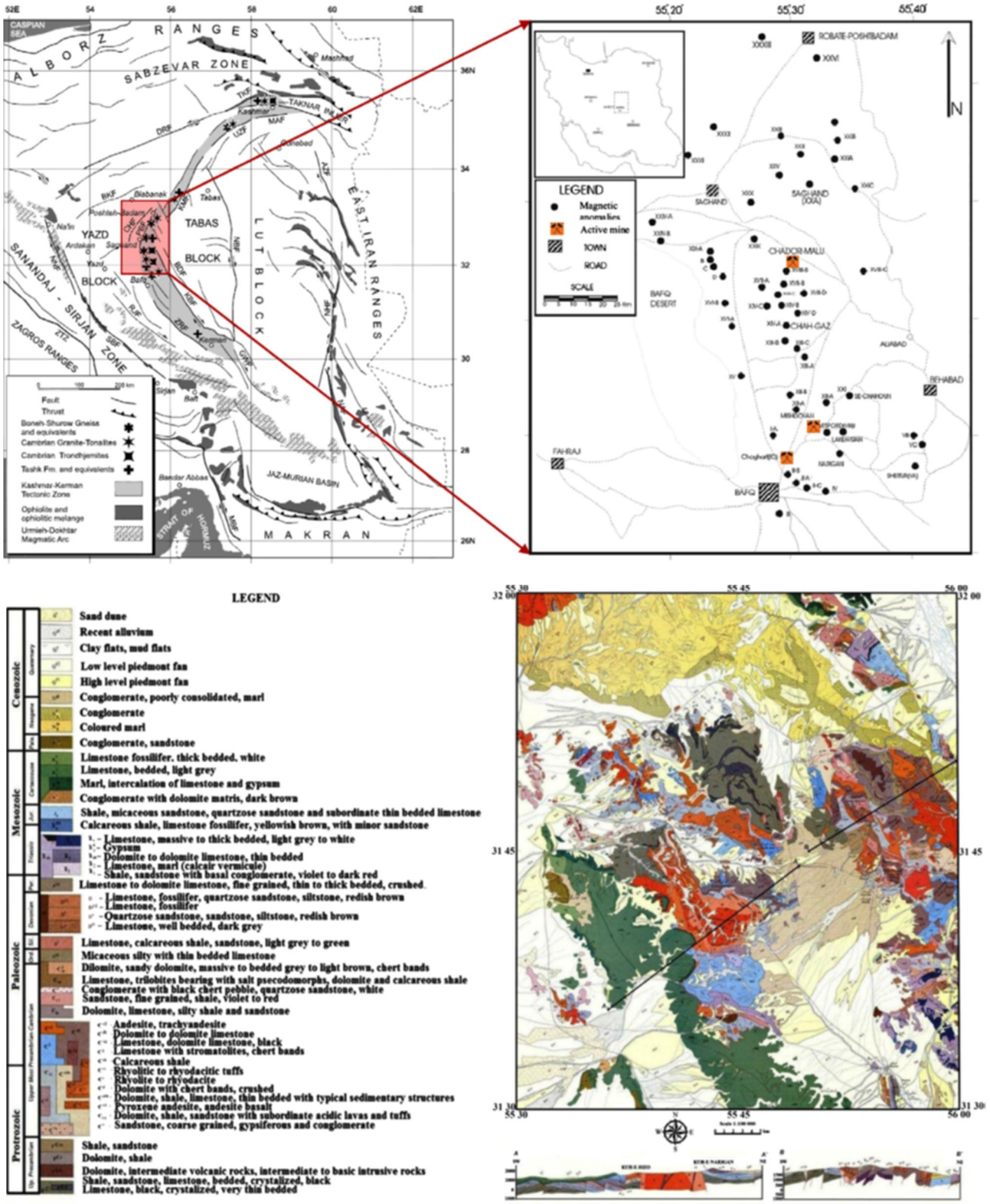

Fig. 1. The metallogenic province of Bafq showing a N–S striking section of the Kashmar–Kerman Tectonic Zone and the location map of the Bafq magnetic occurrences and deposits and the Esfordi deposit [60, 61] and geological map of Esfordi 1:100000 sheet [59].

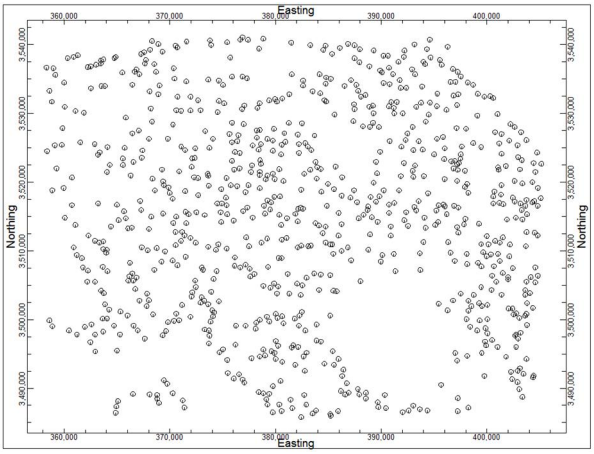

Fig. 2. Samples' location map in the Esfordi 1:100000 sheet

Table 1. Statistical parameters for Fe_2O_3, TiO_2 and V_2O_5 in the Esfordi 1:100000 sheet

	Mean	Median	Maximum	Minimum	Standard Deviation
Fe_2O_3 (%)	5.66	5.00	30.05	3.00	1.74
TiO_2 (%)	0.796	0.78	0.01	1.89	0.17
V_2O_5 (ppm)	86.2	77	705.10	7.00	74.26

This procedure is suggested because it eliminates the undesired smoothing effects caused by usage of Kriging method. Since the IDW method clarifies the ore grade boundaries and ore concentration values, it is more desirable to use IDW method instead of Kriging which inherently has rather high amounts of truncation errors for the upper and lower boundaries of ore grades. The studied area was gridded by 100×100 m2 cells. The cell sizes dimensions were calculated based on geometry of sample collection gridding.

4.1. Factor analysis application

For reduction of variables, factor analysis was performed in the stream sediments geochemical data. The factor analysis was applied and 17 elements and oxides were classified in six factors by using SPSS software to the following groups (Table 2):
(1) Fe_2O_3, TiO_2 and V_2O_5, (2) SiO_2, CaO and B, (3) Ni and Cu, (4) MgO and (5) Li. The first group including Fe_2O_3, TiO_2 and V_2O_5 are important in the area for iron mineralization in the area. For better indication of extracted factors, the factor plot in rotated space is illustrated in Fig. 4.

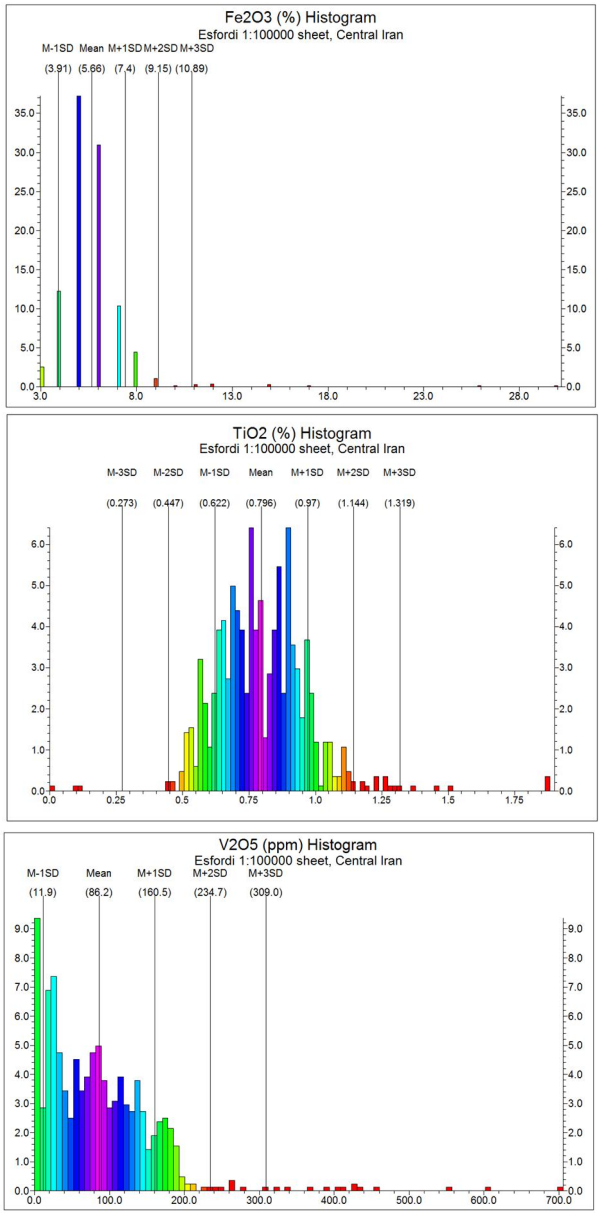

Fig. 3. Fe_2O_3, TiO_2 and V_2O_5 histograms in the Esfordi sheet

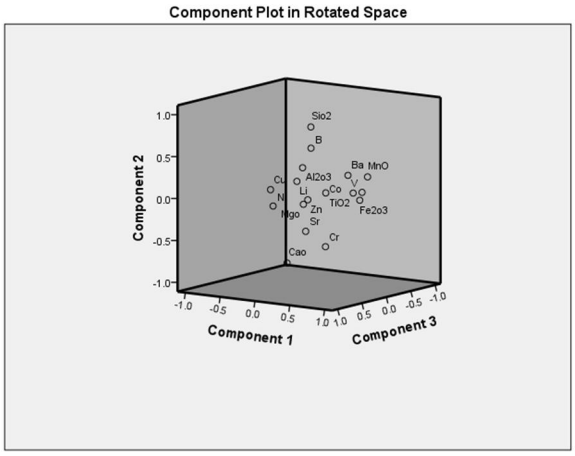

Fig. 4. Component plot in rotated space in the factor analysis

Table 2. Elemental factor analysis in the stream sediment samples from the Esfordi 1:100000 sheet

Rotated Component Matrix[a]

	Component				
	1	2	3	4	5
SiO_2	.044	**.813**	.026	-.130	.133
Fe_2O_3	**.822**	.034	.134	-.048	.148
MgO	-.075	-.123	.009	**.834**	-.163
CaO	-.248	**-.828**	.096	.127	.055
Ni	.028	-.022	**.779**	.187	-.100
Cu	-.011	.168	**.775**	-.049	.113
V_2O_5	**.643**	.066	-.169	-.327	-.147
B	.229	**.617**	.288	.149	-.036
Li	-.119	.156	.079	.099	**.754**
Al_2O_3	-.019	.333	.107	.008	.282
Zn	.190	-.001	.297	.541	.286
Cr	.539	-.506	.433	-.116	.239
Co	.160	.019	-.114	-.020	.383
Ba	.520	.273	-.055	.287	-.079
Sr	.025	-.422	.106	-.140	.556
TiO_2	**.714**	.106	.114	.122	.057
MnO	.588	.217	-.361	.449	.137

4.2. C-N fractal modeling

Based on C-N log-log plots of the elements, there are four geochemical populations for Fe_2O_3 and TiO_2 and six geochemical populations for V_2O_5 respectively (Fig. 5). High intensive anomalies of Fe_2O_3, TiO_2 and V_2O_5 commence from 9.12%, 1.17% and 200 ppm, respectively. However, Fe_2O_3, TiO_2 and V_2O_5 thresholds are 4.46% and 0.64% and 56 ppm, respectively (Table 3). Moreover, C-N log-log plot of first factor was generated which shows five populations (Fig. 5). Main anomalous parts of the Fe_2O_3, TiO_2 and V_2O_5 and related factor were located in the northern, central and western parts of the sheet, as depicted in Fig. 6 which could be prospects for iron ore mineralization. However, high intensive anomalies of V_2O_5 was indicated in the NW part of the area which associated with moderate intensive Fe_2O_3 and TiO_2 anomalies (Fig. 6).

Table 3. Thresholds of Fe_2O_3, TiO_2 and V_2O_5 in Esfordi 1:100000 sheet based on C-N fractal model.

High intensity threshold	Moderate intensity threshold	Low intensity threshold	
9.12	5.75	4.46	Fe_2O_3 (%)
1.17	0.89	0.64	TiO_2 (%)
200	113	56	V_2O_5 (ppm)
3.99	0.80	0.16	F1 (Fe_2O_3, TiO_2, V_2O_5)

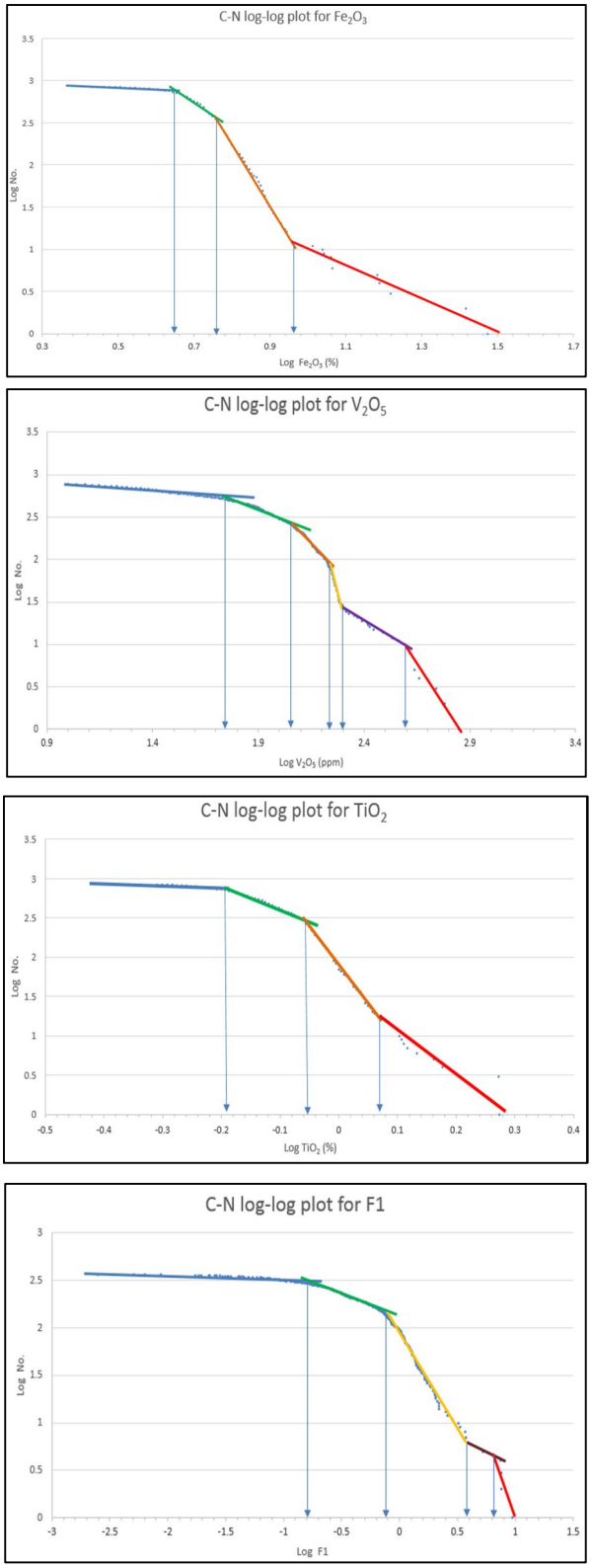

Fig. 5. C-N log-log plots of Fe_2O_3, TiO_2, V_2O_5 and related factor (F1) in the studied area

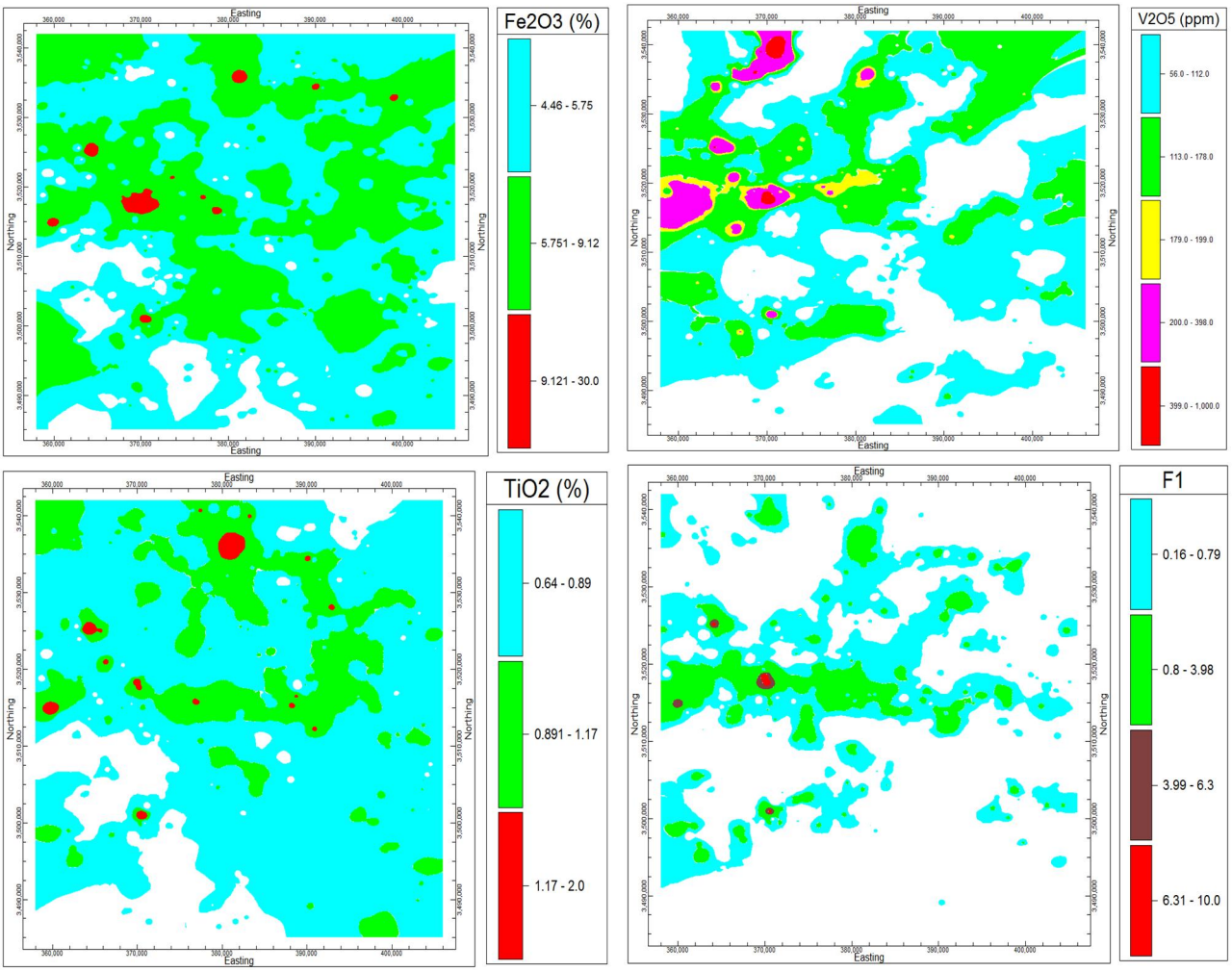

Fig. 6. Geochemical maps obtained by the C-N fractal model of Fe_2O_3, TiO_2, V_2O_5 and first factor (F1) in the studied area

6. Correlation between C-N fractal modeling results and Geological particulars

For validation of the results obtained by C-N fractal modeling, the Fe_2O_3, TiO_2 and V_2O_5 anomalies were correlated with faults and structures, iron alterations and lithological maps. The most parts of these anomalous areas have a good overlap with the structures and faults which determined by remote sensing and geological map (Fig. 7). Faults intersect the anomalies situated near those structures, as depicted in Fig. 7. Main anomalies specifically in the western and central parts of the area associated with iron oxides and alterations which is show in Fig. 8. The high intensive anomalies are near to Esfordi and Choghart iron ores (Fig. 8). Main anomalies in central, western and NW parts of the area accumulated with intrusive and volcanic rocks especially granitic/ryolitic rocks which host main iron ores in the Bafq district (Fig. 9).

Conclusions

The results obtained by this study show that the C-N fractal model is a proper method for separation of different anomalies from background. The classical statistics methods are able to separate only two geochemical populations by median because elemental distribution in most cases are not normal. This process will reduce the accuracy of such studies so utilizing the fractal models could be useful. Moreover, factor analysis could be helped for reduction of variables and separation of multi-elemental anomalies. The results derived via C-N fractal model exhibit Fe_2O_3, TiO_2 and V_2O_5 anomalies in the western, central, NW and northern of the Esfordi area.

Additionally, Main anomalies of Fe_2O_3, TiO_2 V_2O_5 and related factor (F1) obtained by C-N fractal modeling were validated with geological particulars consisting of faults, rock types and iron alterations. The anomalies are correlated with faults and structures especially their intersections. Furthermore, there are granitic/ryolitic intrusive and volcanic rocks which are major host rocks of iron ores in the Bafq region. Moreover, iron

alterations and iron minerals were determined in the anomalous parts based on remote sensing operation. Results of this study indicate that major iron ore prospects illustrate in the central and western parts of the Esfordi area.

Acknowledgements

The paper was extracted from a research project entitled "Reconnaissance of exploration targets for metallic mineralization by integration of airborne magnetometeric, remote sensing and stream sediments geochemical data in Esfordi 1:100000 sheet, Central Iran" by supporting of Islamic Azad University, South Tehran branch. The authors wish to acknowledge the research deputy of Islamic Azad University, South Tehran branch for financial support of this study.

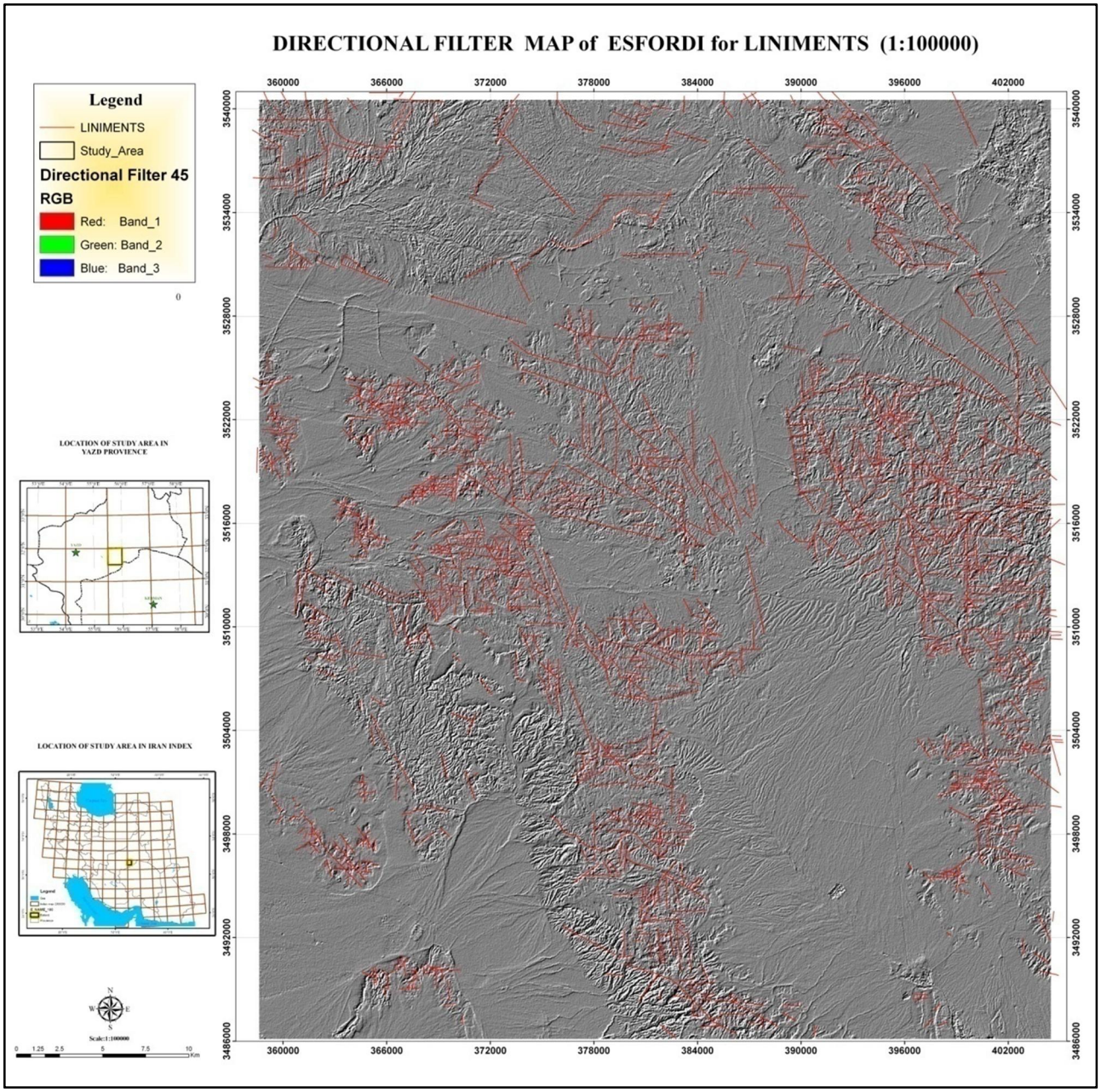

Fig. 7. Correlation between the geochemical anomalies obtained by the C-N fractal model (Yellow ellipsoids) and faults derived via remote sensing and geological map [57] in the Esfordi area.

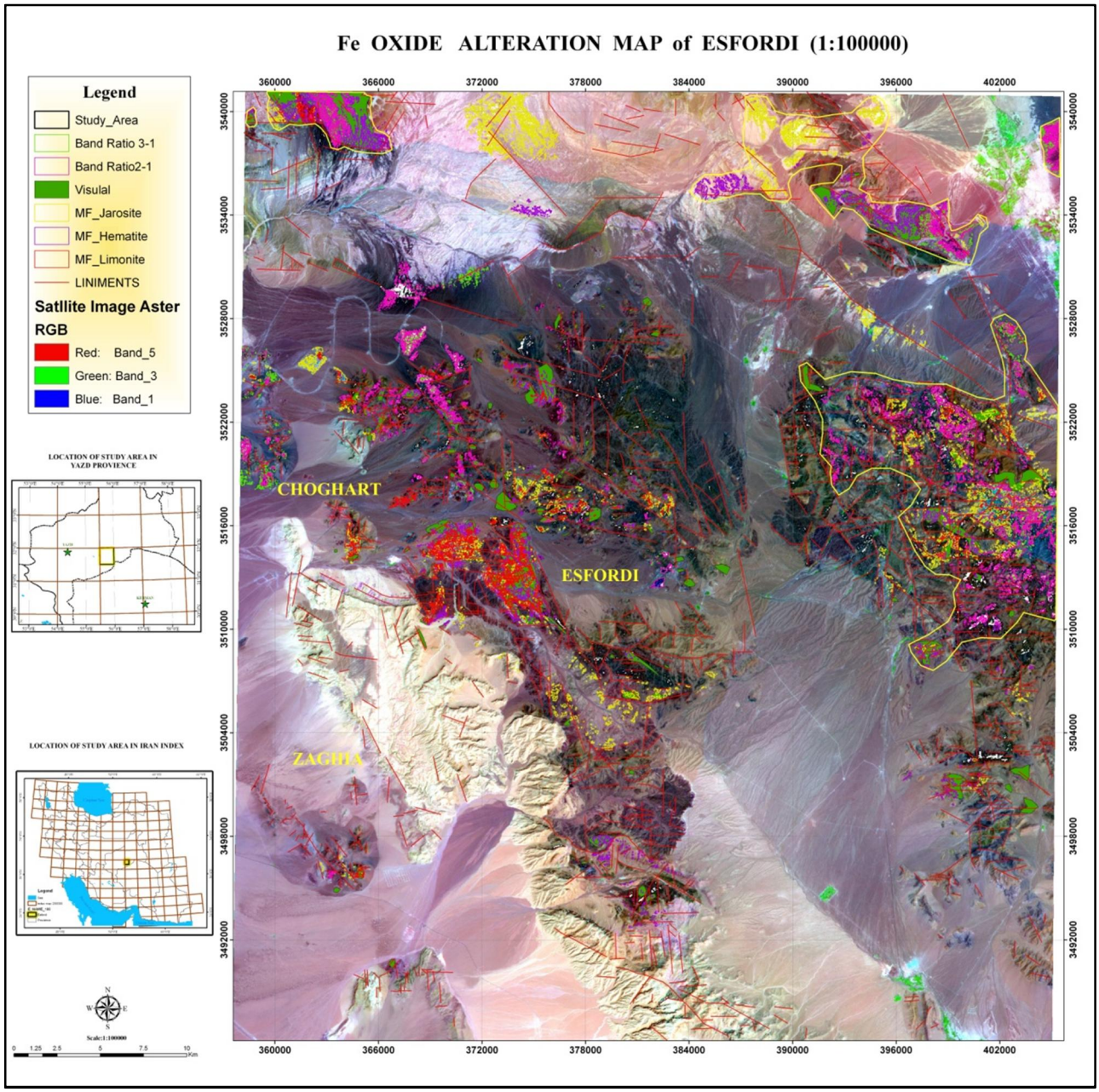

Fig. 8. Correlation between iron alterations resulted from remote sensing methods with main iron ores of the sheet [57] and the geochemical anomalies obtained by the C-N fractal model (Blue ellipsoids).

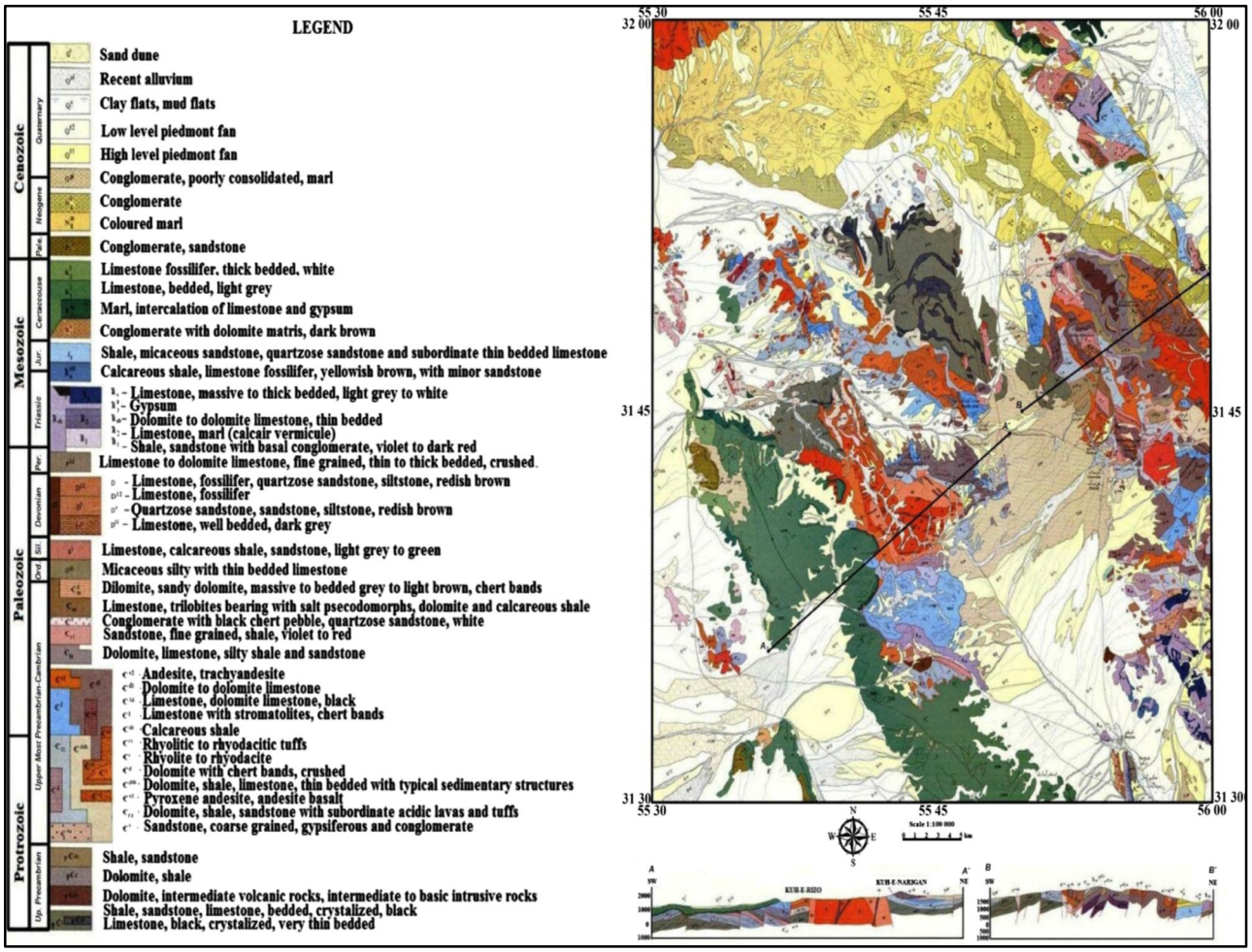

Fig. 9. Correlation between rock types of the sheet [57] and the geochemical anomalies obtained by the C-N fractal model (Blue ellipsoids)

References

[1] Rantitsch, G., 2000. Application of fuzzy clusters to quantify lithological background concentrations in stream-sediment geochemistry. J Geochem Explor 71:73–82.

[2] Grunsky, E.C., Drew, L.J., Sutphin, D.M., 2009. Process recognition in multi-element soil and stream-sediment geochemical data. Appl Geochem 24:1602–1616.

[3] Carranza, E.J.M., 2008. Geochemical Anomaly and Mineral Prospectivity Mapping in GIS. Handbook of Exploration and Environmental Geochemistry, vol 11, Elsevier, Amsterdam, pp 1-351.

[4] Hassanpour, S., Afzal, P., 2013. Application of concentration–number (C–N) multifractal modeling for geochemical anomaly separation in Haftcheshmeh porphyry system, NW Iran. Arab J Geosci 6:957-970.

[5] Deng, J., Wang, Q., Yang, L., Wang, Y., Gong, Q., Liu, H., 2010. Delineation and explanation of geochemical anomalies using fractal models in the Heqing area, Yunnan Province, China. J Geochem Explor 105:95–105.

[6] Pazand, K., Hezarkhani, A., Ataei, M., Ghanbari, Y., 2011. Application of multifractal modeling technique in systematic geochemical stream sediment survey to identify copper anomalies: A case study from Ahar, Azarbaijan, Northwest Iran. Chem Erde 71:397-402.

[7] Zuo, R., 2011. Identifying geochemical anomalies associated with Cu and Pb–Zn skarn mineralization using principal component analysis and spectrum–area fractal modeling in the Gangdese Belt, Tibet (China). J Geochem Explor 111:13-22.

[8] Hawkes, H.E., Webb, J.S., 1962. Geochemistry in Mineral Exploration. Harper and Row, New York, pp 1-415.

[9] Hawkes, H.E., Webb, J.S., 1979. Geochemistry in mineral exploration, 2nd edn. Academic Press, New York, pp 1-657.

[10] Stanley, C.R., Sinclair, A.J., 1989. Comparison of probability plots and gap statistics in the selection of threshold for exploration geochemistry data. J Geochem Explor 32:355–357.

[11] Reimann, C., Filzmoser, P., Garrett, R.G., 2005. Background and threshold: critical comparison of methods of determination. Sci Total Environ 346: 1–16.

[12] Tukey, J.W., 1997. Exploratory Data Analysis. Addison-Wesley Publishing Company, Massachusett, Reading, MA.

[13] Gałuszk, A., 2007. A review of geochemical background concepts and an example using data from Poland. Environ Geol 52(5):861–870.
[14] Yousefi, M., Kamkar-Rouhani, A., Carranza, E.J.M., 2012. Geochemical mineralization probability index (GMPI): A new approach to generate enhanced stream sediment geochemical evidential map for increasing probability of success in mineral potential mapping. J Geochem Explor 115:24-35.
[15] Davis, J.C., 2002. Statistics and data analysis in Geology. John Wiley and Sons Inc, New York, pp 1-638.
[16] Bai, J., Porwal, A., Hart, C., Ford, A., Yu, L., 2010. Mapping geochemical singularity using multifractal analysis: application to anomaly definition on stream sediments data from Funin Sheet, Yunnan, China. J Geochernical Explor 104: 1–11.
[17] Afzal, P., Khakzad, A., Moarefvand, P., Rashidnejad Omran, N., Esfandiari, B., Fadakar Alghalandis, Y., 2010. Geochemical anomaly separation by multifractal modeling in Kahang (GorGor) porphyry system, Central Iran. J Geochem Explor 104:34–46.
[18] Afzal, P., Fadakar Alghalandis, Y., Khakzad, A., Moarefvand, P., Rashidnejad Omran, N., Asadi Haroni, H., 2012. Application of power-spectrum–volume fractal method for detecting hypogene, supergene enrichment, leached and barren zones in Kahang Cu porphyry deposit, Central Iran. J Geochem Explor 112:131-138
[19] Turcotte, D.L., 1986. A fractal approach to the relationship between ore grade and tonnage. Econo Geol 18: 1525-1532.
[20] Agterberg, F.P., Cheng, Q., Wright, D.F., 1993. Fractal modeling of mineral deposits. In: Elbrond J, Tang X (Eds) 24th APCOM symposium proceeding, Montreal, Canada, 43–53.
[21] Agterberg, F.P.,1995. Multifractal modeling of the sizes and grades of giant and supergiant deposits. Int Geol Rev 37:1–8.
[22] Cheng, Q., Agterberg, F.P., Ballantyne, S.B., 1994. The separation of geochemical anomalies from background by fractal methods. J Geochem Explor 51: 109–130.
[23] Bolviken, B., Stokke, P.R., Feder, J., Jossang, T., 1992. The fractal nature of geochemical landscapes. J Geochem Explor 43: 91–109.
[24] Mandelbrot, B.B., 1983. The Fractal Geometry of Nature. WH Freeman, San Francisco, pp 1-468.
[25] Li, C.J., Ma, T.H., Shi, J.F., 2003. Application of a fractal method relating concentration and distances for separation of geochemical anomalie from background. J Geochem Explor 77: 167–175.
[26] Afzal, P., Fadakar Alghalandis, Y., Khakzad, A., Moarefvand, P., Rashidnejad Omran, N., 2011. Delineation of mineralization zones in porphyry Cu deposits by fractal concentration–volume modeling. J Geochem Explor 108: 220–232.
[27] Agterberg, F.P., 2007. Mixtures of multiplicative cascade models in geochemistry. Nonlin Processes Geophys 14: 201–209.
[28] Carranza, E.J.M., 2009. Controls on mineral deposit occurrence inferred from analysis of their spatial pattern and spatial association with geological features. Ore Geol Rev 35: 383-400.
[29] Carranza, E.J.M., Sadeghi, M., 2012. Primary geochemical characteristics of mineral deposits-Implications for exploration. Ore Geol Rev 45: 1–4.
[30] Cheng, Q., 1999. Spatial and scaling modeling for geochemical anomaly separation. J Geochem Explor 65: 175–194.
[31] Cheng, Q., 2008. Modeling local scaling properties for multiscale mapping. Vadose Zone J 7: 525–532.
[32] Zuo, R., Cheng, Q., Xia, Q., 2009. Application of fractal models to characterization of vertical distribution of geochemical element concentration. J Geochem Explor 102: 37–43.
[33] Zuo, R., Xia, Q., 2009. Application fractal and multifractal methods to mapping prospectivity for metamorphosed sedimentary iron deposits using stream sediment geochemical data in eastern Hebei province, China. Geochim Cosmochim Ac 73: A1540-A1540.
[34] Afzal, P., Dadashzadeh Ahari, H., Rashidnejad Omran, N., Aliyari, F., 2013. Delineation of gold mineralized zones using concentration-volume fractal model in Qolqoleh gold deposit, NW Iran. Ore Geology Reviews 55: 125-133.
[35] Goncalves, M.A., Mateus, A., Oliveira, V., 2001. Geochemical anomaly separation by multifractal modeling. J Geochem Explor 72: 91–114.
[36] Lima, A., De Vivo, B., Cicchella, D., Cortini, M., Albanese, S., 2003. Multifractal IDW interpolation and fractal filtering method in environmental studies: an application on regional stream sediments of (Italy), Campania region. Appl Geochem 18(12): 1853–1865.
[37] Zuo, R., Xia, Q., Wang, H. (2013) Compositional data analysis in the study of integrated geochemical anomalies associated with mineralization. Applied Geochem 28: 202-21.
[38] Daneshvar Saein, L., Rasa, I., Rashidnejad Omran, N., Moarefvand, P., Afzal, P., 2012. Application of concentration-volume fractal method in induced polarization and resistivity data interpretation for Cu-Mo porphyry deposits exploration, case study: Nowchun Cu-Mo deposit, SE Iran. Nonliner Processes in Geophysics 19, 431–438.
[39] Daneshvar Saein, L., Rasa, I., Rashidnejad Omran, N., Moarefvand, P., Afzal, P., 2013. Application of number-size (N-S) fractal model to quantify of the vertical distributions of Cu and Mo in Nowchun porphyry deposit (Kerman, SE Iran), Archives of Mining Sciences 58, 1, 89–105.
[40] Muller, J., Kylander, M., Martinez-Cortizas, A., Wüst, RAJ, Weiss D, Blake K, Coles B, Garcia-Sanchez R (2008) The use of principle component analyses in characterizing trace and major elemental distribution in a 55 kyr peat deposit in tropical Australia: implications to paleoclimate. Geochim Cosmochim Ac 72:449–463
[41] Shamseddin Meigoony, M., Afzal, P., Gholinejad, M., Yasrebi, A.B., Sadeghi, B. (2013) Delineation of geochemical anomalies using factor analysis and multifractal modeling based on stream sediments data in Sarajeh 1:100,000 sheet, Central Iran. Arab J Geosci (In press).
[42] Monecke, T., Monecke, J., Herzig, P.M., Gemmell, J.B., Monch, W., 2005. Truncated fractal frequency distribution of element abundance data: a dynamic model forthe metasomatic enrichment of base and precious metals. Earth Planet Sci Lett 232: 363–378.
[43] Sadeghi, B., Moarefvand, P., Afzal, P., Yasrebi, A.B., Daneshvar Saein, L., 2012. Application of fractal models

to outline mineralized zones in the Zaghia iron ore deposit, Central Iran. J Geochem Explor, Special Issue "fractal/multifractal modelling of geochemical data", 122: 9-19.
[44] Sanderson, D.J., Roberts, S., Gumiel, P., 1994. A Fractal relationship between vein thickness and gold grade in drill core from La Codosera, Spain. Econ Geol 89: 168–173.
[45] Shi, J., Wang, C., 1998. Fractal analysis of gold deposits in China: implication for giant deposit exploration. Earth Sciences Journal of China University of Geosciences 23: 616–618 (In Chinese with English Abstract).
[46] Turcotte, D.L., 1997. Fractals and Chaos in Geology and Geophysics. Cambridge University Press, Cambridge, pp 1-398.
[47] Wang, Q.F., Deng, J., Wan, L., Zhao, J., Gong, Q.J., Yang, L.Q., Zhou, L., Zhang, Z.J., 2008. Multifractal analysis of the element distribution in skarn-type deposits in Shizishan Orefield in Tongling area, Anhui province, China. Acta Geol Sin 82: 896–905.
[48] Mohammadi, A., Khakzad, A., Rashidnejad Omran, N., Mahvi, M.R., Moarefvand, P., Afzal, P., 2013. Application of number-size (N-S) fractal model for separation of mineralized zones in Dareh-Ashki gold deposit, Muteh Complex, Central Iran. Arab J Geosci 6: 4387-4398.
[49] Hashemi, M., Afzal, P., 2013. Identification of geochemical anomalies by using of number-size (N-S) fractal model in Bardaskan area, NE Iran. Arab J Geosci 6: 4785–4794.
[50] Tripathi, V.S., 1979. Factor analysis in geochemical exploration. J Geochem Explor 11: 263–275.
[51] Jolliffe, I.T., 2002. Principal Component Analysis, 2nd edn. Springer, New York, pp 1-487.
[52] Johnson, R.A., Wichern, D.W., 2002. Applied Multivariate Statistical Analysis, 5th edn, Prentice Hall, New Jersey.
[53] Krumbein, W.C., Graybill, F.A., 1965. An Introduction to Statistical Models in Geology. McGraw-Hill, New York.
[54] Haghipour, A., 1977. Geological map of Posht-e-Badam area. Geol Surv Iran.
[55] Samani, B.A., 1988. Metallogeny of the Precambrian in Iran. Precambrian Research 39: 85-106.
[56] Forster, H.G., Jafarzadeh, A., 1994. The Bafq mining district in central Iran; a highly mineralized Infracambrian volcanic field. Economic Geology 89: 1697-1721.
[57] Daliran, F, Stosch, H.G, Williams, P., Jamli H., Dorri, M.B., 2010. Early Cambrian Iron Oxide–Apatite–REE (U) Deposits of the Bafq District, East–Central Iran. In: Corriveau L, Mumin H (eds) Exploring for Iron oxide copper–gold deposits: Canada and Global analogues. Geol Assoc Canada, Short Course Notes 20, p.p. 143–155.
[58] Stosch, H.G., Romer, R.L., Daliran, F., Rhede, D., 2011. Uranium–Lead ages of apatite from iron oxide ores of the Bafq District, East-Central Iran, Miner Deposita 46: 9–21.
[59] Sadeghi, B., Khalajmasoumi, M., Afzal, P., Moarefvand, P., Yasrebi, A.B., Wetherelt, A., Foster, P., Ziazarifi, A., 2013). Using ETM+ and ASTER sensors to identify iron occurrences in the Esfordi 1:100000 mapping sheet of Central Iran. Journal of African Earth Sciences 85: 103-114.
[60] Ramezani, J., Tucker, R.D., 2003. The Saghand region, Central Iran: U–Pb Geochronology, Petrogenesis and Implications for Gondwana Tectonics, Amer J Sci 303: 622–665.
[61] Jami, M., 2005. Geology, Geochemistry & Evolution of Esfordi Phosphate (Iron Deposit, Bafq Area – Central Iran), Unpublished Ph.D thesis, University of New South Wales, 384 p.